

Femtosecond laser photodisruption of human trabecular meshwork: an in vitro study

Sami Toyran^a, Yaoming Liu^b, Sima Singha^b, Sun Shan^c, Michael R. Cho^c,
Robert J. Gordon^b, Deepak P. Edward^{a,*}

^aDepartment of Ophthalmology and Visual Sciences (m/c 648), University of Illinois at Chicago, Chicago, IL 60680, USA

^bDepartment of Chemistry (m/c 111), University of Illinois at Chicago (m/c 111), Chicago, IL 60680, USA

^cDepartment of Bioengineering (m/c 063), University of Illinois at Chicago, Chicago, IL 60680, USA

Received 17 August 2004; accepted in revised form 3 February 2005

Available online 17 March 2005

Abstract

The goal of this in vitro study was to test the feasibility of using femtosecond (fsec) laser pulses to fistulize the human trabecular meshwork (TM), and to determine the minimum exposure time and energy dosage needed to create an ablation channel. Corneo-scleral rims were obtained from tissue used for penetrating keratoplasty. Four millimeter tissue strips hydrated in Optisol-GS were used to create partial thickness fistulas in the human TM by focusing a Ti:Sapphire laser beam (45 fsec, 1 kHz, 800 nm) with various pulse energies (7.2 and 14.4 μJ) and exposure times (0.25, 0.5, 1, and 2 sec) on the inner surface of the TM. Two-photon images of the lesions were obtained with a multiphoton microscope, using an ultrafast Ti:Sapphire light source. In addition, sections of fixed tissue were examined by light microscopy. Diameters and lengths of the lesions were determined from the hematoxylin and eosin (H&E) stained sections, and the collagen structure surrounding the lesion was evaluated from the two-photon images.

All selected time points (except for 0.25 sec) and energies achieved the desired photodisruption of the TM. Incisions created with 0.5 sec/14.4 μJ irradiation appeared to be the most suitable because they were able to achieve consistent full thickness trabecular ablation. Incisions created at 1 sec/14.4 μJ/pulse and 2 sec/14.4 μJ/pulse were deeper than those at shorter time points with the same pulse energy. Longer exposure times and higher pulse energies were usually more variable and associated with deeper and larger incisions and slight collateral damage.

Our results indicate that, with appropriate exposure time and pulse energy, fsec photodisruption can be employed to create lesions in the human TM without damaging the surrounding tissues. This study demonstrates that fsec laser treatments may have future potential for the surgical treatment of glaucoma.

© 2005 Elsevier Ltd. All rights reserved.

Keywords: femtosecond laser; trabecular meshwork; laser sclerostomy; laser trabecular ablation

1. Introduction

Conventional glaucoma surgical techniques stimulate fibrosis and scarring, which can subsequently lead to the closure of the surgically created fistula. Although recent research has focused on drug development, there is a great need for a simple noninvasive surgical procedure to treat

glaucoma. The goal of this study is to determine if fsec laser irradiation can be used to create an ablation channel consistent with reduction of intraocular pressure without causing damage to surrounding tissues. Ultrashort laser pulses have the remarkable capability of ablating biological tissue while causing little collateral damage. The origin of this behaviour is the localized plasma produced by the intense laser field, which ablates material before thermal and mechanical relaxation occurs.

Previous attempts at laser trabecular ablation (LTA) used Nd:YAG, Er:YAG, and XeCl excimer lasers. These treatments were ineffective or not widely accepted, either because of laser-induced thermal damage or because of the need for complex laser delivery systems that made it

* Corresponding author. Dr Deepak P. Edward, Department of Ophthalmology and Visual Sciences, University of Illinois at Chicago, 1855 West Taylor Street, L 217, Chicago, IL 60612, USA.

E-mail address: deepedwa@uic.edu (D.P. Edward).

difficult to create consistent and reproducible results. The primary reason for the failure of LTA is that all of the studies to date relied mainly on a thermal ablation mechanism (Melamed et al., 1987; Hill et al., 1993; Dietlein et al., 1997, 2001; Vogel and Venugopalan, 2003). For pulse durations of several nanoseconds or longer, thermal and mechanical relaxation occur during the pulse and compete with material ablation (Niemz, 2002). In these studies, very large pulse energies (on the order of several mJ) were used to achieve sufficient local penetration to ablate the tissue. Ultrashort (sub-picosecond) pulses, on the other hand, confine the thermal and mechanical stresses to a localized volume. Depending on the properties of the tissue, a significant amount of material may be ablated before thermal diffusion, shock propagation, and cavitation can occur. In this case, thermal and mechanical collateral damage are reduced. An objective of the present study is to determine the extent of collateral damage produced by fsec LTA.

2. Materials and methods

2.1. Laser and delivery system

A schematic drawing of the apparatus is given in Fig. 1. A regeneratively amplified Ti:Sapphire laser was used to generate the fsec pulses. Seed pulses were generated with a Spectra Physics Tsunami oscillator, operating at a peak wavelength near 800 nm. These pulses were amplified with a Spectra-Physics Spitfire regenerative amplifier to produce 2 mJ, 45 fsec pulses at a 1 kHz repetition rate. The output from the amplified laser was directed through a half wave plate and polarizer for precise control of the pulse energy.

The pulse energy was measured after the focusing optics with an Ophir 2A-SH power meter. The attenuated laser beam was reflected by a pair of periscope mirrors into the objective of a modified microscope fitted with either a 4×/NA 0.12 or a 10×/NA 0.25 objective lens. Most of the experiments were performed with the 0.25 NA objective, which was mounted in the microscope so that the tissue could be observed concurrently, using a beam splitter and eyepiece. The focal parameters of the laser beam were measured using a scanning knife edge and photodiode. It was found that when the laser was focused with just the objective lens, the beam had a clean Gaussian profile, with a radius (defined at the point where the intensity drops by $1/e^2$) of $\omega_0 = 2.9 \mu\text{m}$ and a Rayleigh range of $z_0 = 12.7 \mu\text{m}$, giving a ratio of $\omega_0/z_0 = 0.226$ (in reasonable agreement with the lens NA). It was observed, however, that the beam splitter distorted the shape of the focused beam and increased the focal radius to approximately $20 \mu\text{m}$. We estimate that the combined optics of the microscope stretched the laser pulse to 75 fsec.

The tissue to be treated was mounted on a three dimensional translation stage, which could be positioned with $0.5 \mu\text{m}$ precision along each axis. The TM could be identified by the experimenter in situ using the eyepiece of the modified microscope. The stage was then repositioned to bring the focus of the laser just below the tissue surface. Two pulse energies (7.2 and 14.4 μJ) and varying exposure times (0.25, 0.5, 1 and 2 sec) were used to ablate the tissue. The exposure time was controlled precisely using a computer to trigger the Pockels cell of the laser amplifier. The lesions produced by the lasers were clearly visible through the focused eyepiece. The procedure was done in room air, but during the procedure the tissue was kept wet using the Optisol solution.

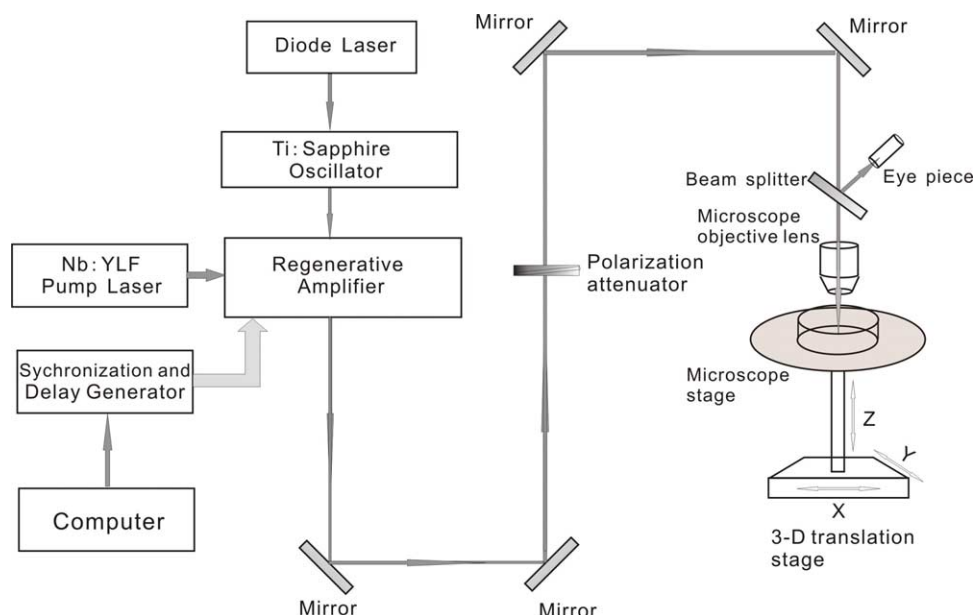


Fig. 1. The experimental setup for laser ablation of tissues.

2.2. Tissue

Corneo-scleral rims were obtained from donor tissue remaining after penetrating keratoplasty. The procurement of tissues was approved by the Institutional Review Board at the University of Illinois at Chicago and complied with the Declaration of Helsinki. These rims, stored in Optisol-GS, were used within a week from the time of death. The tissue was examined under a dissecting microscope for presence of TM and cut radially into several 4 mm wide pieces. Schlemm's canal was marked at the edge of the tissue using a dye to make the TM easily identifiable during laser delivery. The areas ablated were not stained with the dye. Multiple laser parameters were investigated with variable laser energy and exposure times. Three to four lesions using the same laser parameters were produced on each tissue strip.

2.3. Microscopy

Two-photon images of the TM, with and without LTA, were acquired using a BioRad Multiphoton microscope. Multiphoton fluorescence microscopy utilizes two-photon excited fluorescence and second harmonics generated from collagen and similar molecules to provide a tool to image structure within the TM (Konig, 2000; Zoumi et al., 2002; Campagnola and Loew, 2003; Mohler et al., 2003; Zipfel et al., 2003). The advantage of the two-photon imaging used in this study was that we were able to obtain accurate dimensions of thick sections without the shrinkage effect of fixation.

Some samples were treated with diamidinophenylindole (DAPI) to label the nuclei in the TM. All samples were irradiated with the output of a Ti:sapphire oscillator (750 nm, 80 fsec, 1.2 nJ/pulse, 82 MHz), focused with a 60×1.3 NA oil immersion objective, and scanned with a resolution of 0.1–0.3 μm to produce the image. Superficial and deep components of the lesion were measured with the help of the Metamorph Image Analyzer (Universal Imaging Corporation; West Chester, PA). These images were also used to qualitatively assess the collateral damage to the collagen fibers and trabecular endothelial cells in the uveal and corneo-scleral TM.

The laser treated tissues were then fixed in 4% buffered formaldehyde and processed for paraffin embedding. Serial 5 μm sections were cut and stained with H&E. The tissues were examined for the presence of laser lesions, and their dimensions were recorded. The length and width of the laser lesion through the TM were measured at its greatest length of penetration into the tissue. These measurements were made using a Zeiss microscope, using Axioskop 2 Plus software with the Metamorph Image Analyzer.

Table 1
Dimensions of the ablated lesions

Pulse energy (μJ)	Exposure time (sec)	Number of samples	Width (μm)	Length (μm)
7.2	0.5	3	11.0 ± 1.6 ^a 28/8 ^b	50.4 ± 3.4 ^a
	1	3	21.8 ± 5.7 ^a 33/14 ^b	71.6 ± 20.7 ^a
	2	3	22.3 ± 1.0 ^a 34/15 ^b	87.7 ± 1.4 ^a
14.4	0.5	12	33.5 ± 7.8 ^a 34/20 ^b	82.1 ± 23.6 ^a
	1	12	36.4 ± 10.3 ^a 43/25 ^b	153.0 ± 16.2 ^a
	2	4	50.8 ± 20.9 ^a 45/33 ^b	197.9 ± 13.3 ^a

^a Data obtained from histological sections.

^b Data obtained from two-photon images. The first entry is the superficial diameter; the second is the diameter ~100 μm beneath the surface.

3. Results

The lengths and diameters of the lesions created by fsec LTA at two pulse energies (7.2 and 14.4 μJ) are summarized in Table 1. Histological sections are shown in Fig. 2, and superficial two-photon images are shown in Fig. 3. Deep two-photon images are shown in the insets of Fig. 3. More lesions were studied at near optimal conditions to assure consistency in the tissue response.

3.1. Laser lesions with 7.2 μJ

As observed with light microscopy, most of the LTA lesions penetrated the entire length of the meshwork at each time point (Fig. 2, lesions 1, 2, and 3). At shorter exposure times (0.5 sec) the laser was not always able to penetrate the entire thickness of the meshwork, and penetration appeared to depend on the location of application in the TM (anterior or posterior). The margins of the lesions were sharp, and no collateral damage was noted. The edges of the lesions at this energy level were mostly parallel, but 'barrel' and conical shaped lesions were occasionally noted. The well demarcated margins were confirmed by two-photon imaging, which showed oval to round laser-induced cuts through collagen without coagulative damage or fraying of fibers and preservation of the trabecular endothelial cell nuclei through superficial and deep aspects of the lesion at all exposure times, except at 2 sec exposure where mild coagulative damage was seen at the edge of the lesion (Fig. 3, left top, middle, and bottom).

As the exposure time increased from 0.5 to 2 sec, an increase in the length and width of trabecular ablation was noted. In the H&E sections, the average widths increased from 11 to 22 μm and the lengths increased from 53 to 88 μm. The two-photon images consistently showed a smaller width deep in the tissue, indicating a tapering of the lesion (Table 1). No laser-induced lesions were

identified at an exposure time of 0.25 sec. Of note is that the lesion diameter obtained on the surface by two-photon imaging was consistently larger than that obtained on the tissue sections.

3.2. Laser lesions with 14.4 μJ

At this energy level the appearance of the lesion at 0.5 sec (Fig. 2, lesion 4) was similar to, but larger than, that obtained with 7.2 μJ . At 1 and 2 sec, however, the lesion appeared more conical in shape and penetrated the outer wall of Schlemm's canal (Fig. 2, lesions 5 and 6). Also, thermal damage was noted at the edges of the lesion at 2 sec exposure time (Fig. 2, lesion 6). The lesion dimensions were fairly consistent and reproducible. As noted with lower energy lesions, two-photon imaging with DAPI staining confirmed the findings seen with light microscopy. There was an absence of thermal damage to the tissue at 0.5 and 1 sec exposure times (Fig. 3, right top and middle). At 2 sec exposure time mild coagulative damage was noted at the edges of the lesion in the deeper aspect as indicated with arrowheads (Fig. 3, inset, bottom right).

The increase in lesion dimensions with time is evident at this energy. The average width increased from 33 to 51 μm , and the length grew from 82 to 198 μm , when the exposure time was increased from 0.5 to 2 sec. The two-photon images showed a comparable increase in width, and again indicated a tapering of the lesion within the tissue. An increase in variability in lesion width was noted with increase in exposure time, and this variability appeared to be larger than that seen with 7.2 μJ (Table 1). No lesions were observed at an exposure time of 0.25 sec. As with the laser induced lesions at 7.2 μJ , the lesion diameter with the two-photon imaging was consistently larger than that obtained on H&E tissue sections.

4. Discussion

4.1. Properties of femtosecond laser ablation

Femtosecond lasers are a promising tool for micromachining of biological tissue (Lubatschowski et al., 2002). There are three fundamental advantages in using ultrashort

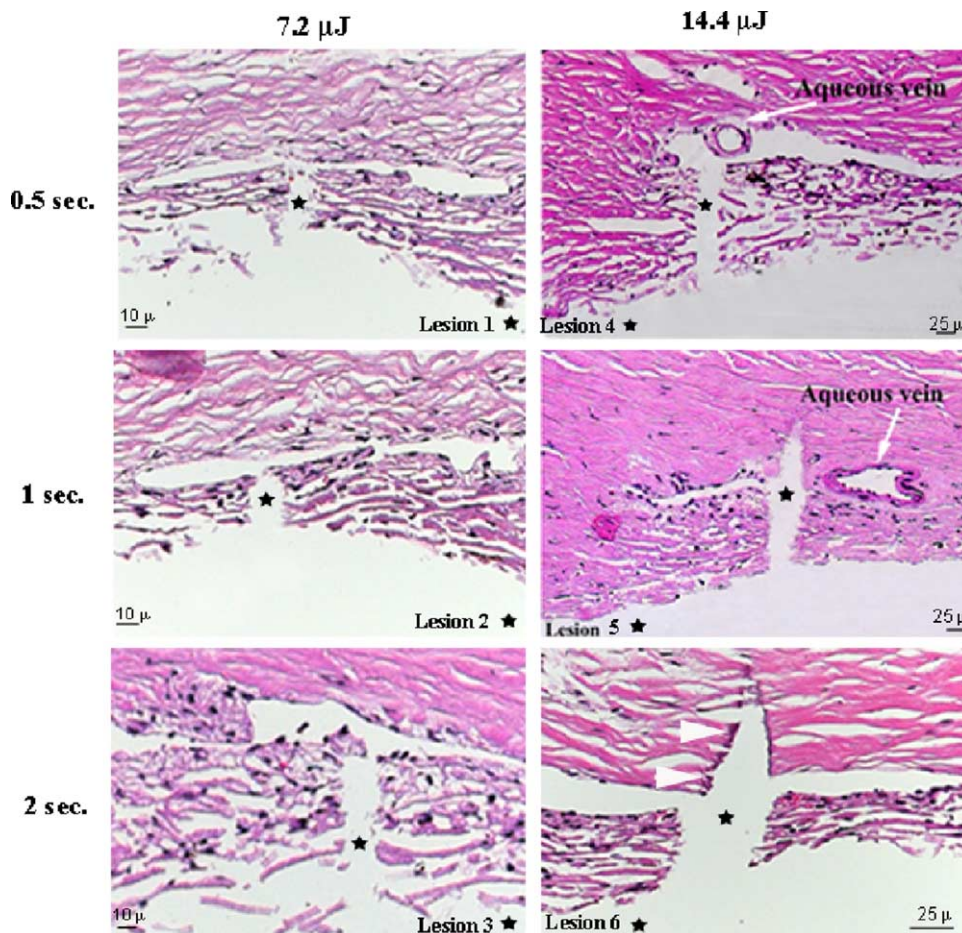


Fig. 2. Microphotographs showing histology of fsec LTA lesions in the human trabecular meshwork. Average dimensions of the lesions are given in Table 1. Lesions 1, 2, and 3: fsec LTA at a pulse energy of 7.2 μJ at varying durations (0.5, 1, and 2 sec, respectively). Note the sharp margin of the lesions through the TM and into Schlemm's canal and preservation of the outer wall of the canal. Lesions 4, 5, and 6: fsec LTA lesions at a pulse energy of 14.4 μJ at varying durations (0.5, 1, and 2 sec, respectively). Note the size and collateral damage of the lesion with the higher dose (arrowheads). (H&E; original magnification, 20 \times).

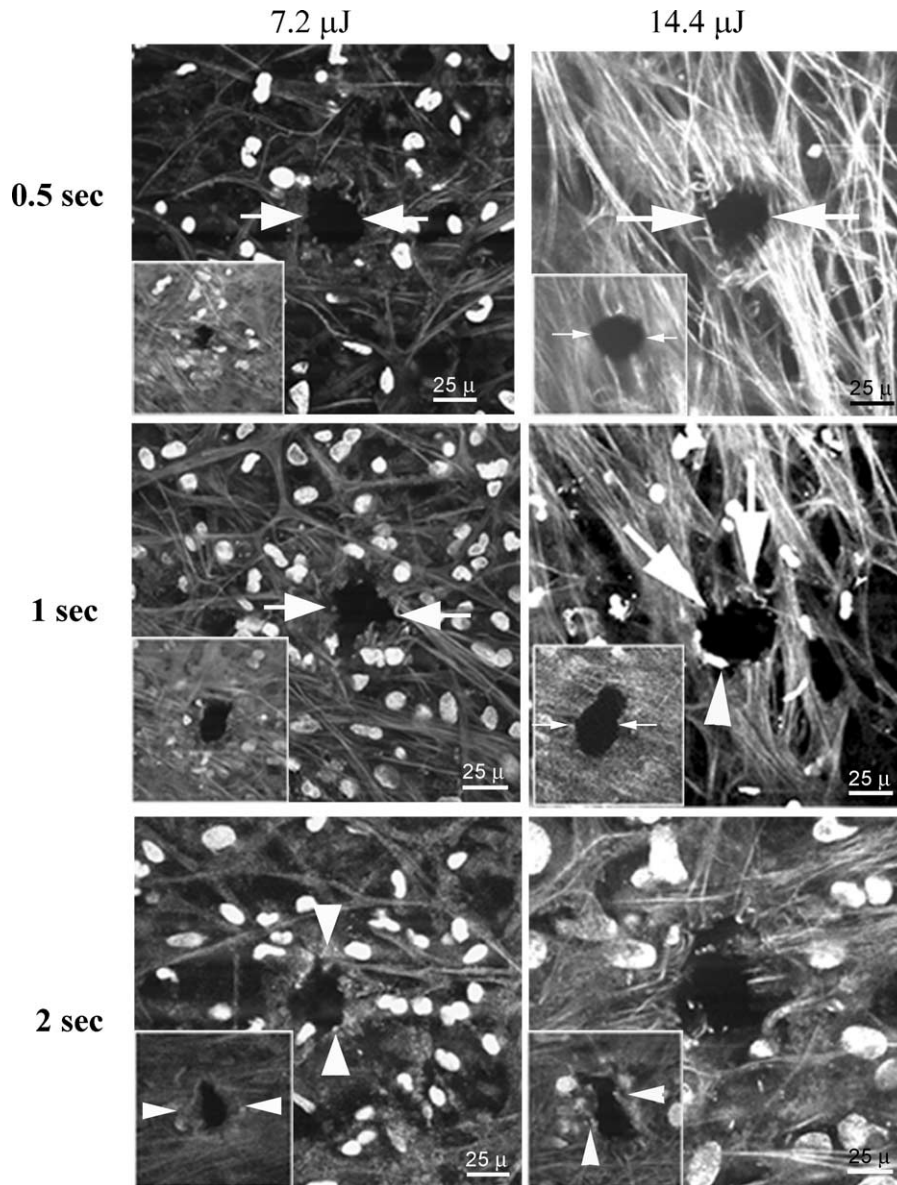


Fig. 3. Two-photon images of the ablated TM, recorded with 750 nm radiation. The primary image in each panel is taken at the surface of the tissue in the uveal meshwork, and the inset is an image in the deep tissue at or close to the level of the corneoscleral meshwork section deep in the tissue. The left panel shows the LTA lesions using a pulse energy of 7.2 μJ at 0.5, 1 and 2 sec duration, respectively. Nuclear labeling with DAPI shows preservation of the nuclei surrounding the lesions. Note the distinct fibers on the surface uveal meshwork and in the deep meshwork, demonstrating the clean-cut margins of the fsec LTA lesion with minimal collateral damage (left bottom, arrowheads) and absence of thermal coagulation (left top, middle, arrows). The right panel shows the fsec LTA lesions using a pulse energy of 14.4 μJ at 0.5, 1 and 2 sec duration, respectively. Note the nuclear labeling with DAPI (right, middle panel, arrowhead) showing preservation of the nuclei at the edge of the lesion. Also note the absence of thermal coagulation in the 0.5 and 1 sec lesions (arrows, top and middle panel). Mild thermal coagulative damage of the collagen is noted in the deeper tissue at 2 sec (right panel inset; bottom, arrowheads). Excitation wavelength of TPE: 750 nm, pulse width: 80 fsec, excitation pulse energy: 1.58 nJ, objective lens: 60 \times oil.

Ti:Sapphire lasers for ablation, as compared with long pulse lasers. First, the 800 nm wavelength of the Ti:Sapphire laser falls within the absorption window of most tissues, allowing radiation to be focused to a point within the target without damaging the outer layers (e.g. the cornea). Second, the short length causes the radiant energy to be absorbed on a time scale that is much shorter than both thermal diffusion and shock wave propagation. This property leads to thermal and stress confinement, thereby reducing

the region of material damage to the vicinity of the laser focus. Third, the lower fluence threshold for fsec ablation reduces the overall thermal and mechanical load on the tissue (Vogel and Venugopalan, 2003).

Most of the advantages of ablation with the fsec Ti:Sapphire laser stem from its unique excitation mechanism. Ablation with a long pulse or continuous wave laser is a linear (i.e. single photon) process. The penetration depth is determined by the absorption coefficient at the laser

wavelength. For visible and infrared wavelengths, material disruption is caused entirely by thermal and mechanical dissipation of energy. With UV radiation part of the ablation is caused by direct photochemical bond breaking, but, because of the long pulse duration (typically 15 ns), thermal and mechanical relaxation compete with tissue evaporation (Vogel and Venugopalan, 2003). Moreover, for the 308 nm excimer laser that has been used for LTA (Vogel and Lauritzen, 1997), very little photochemical decomposition of protein has been reported, with $\sim 80\%$ of the energy converted directly to heat (Oraevsky et al., 1996). In contrast, ultrafast lasers rely on a nonlinear (i.e. multiphoton) mechanism. Five 800 nm photons must be absorbed to overcome the water bandgap, and an additional five photons are required to initiate an electron avalanche. This avalanche leads to optical breakdown, and the resulting plasma mediates the ablation process. Because a high intensity is required to absorb so many photons, the breakdown is confined to a small volume near the focal point (Oraevsky et al., 1996).

Although thermal and mechanical propagation can and do occur after the fsec laser pulse, there are at least three factors that mitigate the extent of collateral damage. First, the fluence threshold for optical breakdown (and therefore for ablation) decreases nonlinearly with pulse duration. In water, for example, the breakdown threshold decreases from 150 J cm^{-2} at 10 ns to 1 J cm^{-2} at 75 ns (Vogel and Venugopalan, 2003). A similar dependence has been observed for collagen (Oraevsky et al., 1996). The much higher breakdown thresholds for longer pulse lasers imply that they rely on an absorption mechanism for ablation. Second, the multiphoton infrared excitation that initiates the plasma can also cause photochemical bond breaking before energy relaxation occurs. Third, it was observed in collagen that the very high mechanical frequencies excited by an ultrashort pulse impede shock wave propagation, thereby reducing stress on the surrounding material (Oraevsky et al., 1996).

4.2. Application to laser trabecular ablation

This study demonstrates the feasibility of using a modified microscope delivery system for LTA and the ability to ablate the TM using fsec pulses in a dose-dependent fashion. The ideal LTA lesion is one that penetrates the TM and the inner wall of Schlemm's canal and has a diameter sufficient for aqueous outflow without leading to collateral damage. In this series of experiments we were able to ablate the TM without damage to the outer wall of Schlemm's canal. Very low pulse energies were required, and we were able to demonstrate precise and reproducible cutting effects. Histological examination of the LTA lesions revealed sharply demarcated edges, with no thermal damage at $7.2 \text{ } \mu\text{J/pulse}$ and slight damage for 2 sec exposure at $14.4 \text{ } \mu\text{J/pulse}$. These results were confirmed by two-photon imaging. We estimate that, with the distortions

produced by the microscope optics, the fluence at the focal point was 1 and 2 J cm^{-2} at the two pulse energies, respectively. We did observe mild collateral damage to the collagen at high energy settings, and it is possible that in the living eye with limited flow in the anterior chamber, increased collateral damage may result from cavitation. An option to avoid collateral damage might be to reduce the pulse energy by continuously refocusing the laser as the irradiation progresses, using a computerized motor drive attached to the objective lens. This procedure would have the added advantage of producing a more uniform diameter along the length of the ablation channel.

Previous studies of LTA used Nd:YAG, Er:YAG, and XeCl excimer lasers. In general, the energy levels and fluence used for LTA with the fsec laser in this study was lower than that for other lasers. For the Nd:YAG laser (1064 nm, 5–7 mJ/pulse, 14 ns pulse duration; fluence: $1.5\text{--}2.2 \text{ J cm}^{-2}$), the amount of energy necessary to create the sclerostomy caused significant trauma to adjacent tissues (Melamed et al., 1985). In this case it was difficult to determine the consistency of the lesions created by the laser. In an in vitro study of Nd:YAG laser trabeculotomy, Venkatesh et al. (1986) produced $100 \text{ } \mu\text{m}$ lesions (30 mJ/pulse ; 40–50 ns pulse duration) that penetrated Schlemm's canal with only minimal damage to adjacent tissue. But scanning electron microscopy showed that there was considerable variation in the size of the lesions. They proposed that there was no correlation between the dimensions of the laser-induced lesion and the laser operating parameters.

In vitro studies with an Er:YAG laser ($2.94 \text{ } \mu\text{m}$, 2–7 mJ/pulse, 200–250 μs pulse duration; fluence: $14\text{--}28 \text{ J cm}^{-2}$) demonstrated (McHam et al., 1992) less collateral thermal damage than that seen with the Nd:YAG laser. The thermal damage began at 50 μs and was found to be directly proportional to the exposure time. On the other hand, when the exposure time was reduced, the ablation area became less predictable and varied in size from 0 to $140 \text{ } \mu\text{m}$ (Hill et al., 1993). Dietlein et al. (1996) found that the diameter of the ablation crater increased from 133 to $173 \text{ } \mu\text{m}$ when the pulse energy was increased from 4 to 6 mJ (fluence: 6 J cm^{-2}). Furthermore, Er:YAG treatment in rabbits resulted in an acute inflammatory response, leading to damage to the outer wall of Schlemm's canal and fibrous scarring that blocked aqueous outflow, similar to that seen in monkeys following Nd:YAG LTA. Also noted in both studies was the obliteration of the trabecular beams by scar tissue and endothelial proliferation within 60 days (Dietlein et al., 1997).

The diameter of the lesions created by the ARF excimer laser used for sclerostomy (193 nm, 17–28 mJ, $\sim 15 \text{ ns}$; fluence: 0.4 J cm^{-2}) was approximately $300 \text{ } \mu\text{m}$ (Allan et al., 1993). Vogel and colleagues demonstrated increased outflow facility in an in vitro study using a XeCl excimer laser (308 nm, 4.4–6.9 mJ, $\sim 15 \text{ ns}$; fluence: $3.5\text{--}5.5 \text{ J cm}^{-2}$), and showed modest intraocular pressure

lowering (median 7 mmHg) at 7 months, using an intraocular 400 μm quartz fiber to create 4–5 pores in an in vivo study (Vogel and Lauritzen, 1997). Huang et al. (2001) showed minimal trabecular scarring in a rabbit model of ab interno excimer LTA. In principle, such excimer laser-induced LTA lesions might be ideal, although certain limitations are evident because of the need to use an intraocular probe to create LTA with UV radiation.

Tissue removal may be understood in terms of an optical or a ‘blow off’ model, in which successive layers are removed by laser pulses, with the dimensions of the ablated area determined by the spatial profile of the laser beam without thermal damage (Deutsch and Geis, 1983; Vogel and Venugopalan, 2003). The lesion diameters produced in the present study at ~ 20 and ~ 40 times the ablation threshold are consistent with those findings. The penetration depth of an oncoming laser pulse is limited to a few micrometer because of the high reflectivity of the plasma. Material near the surface of an area recently ablated is subject to the greatest heating from earlier pulses, which lowers the ablation threshold and thereby broadens the crater. Because the fluence decreases with the square of the axial distance from the focal point, the ablation efficiency decreases rapidly with depth, requiring higher fluence and longer exposure time to achieve a desired channel length. Moreover, the plasma produced by optical breakdown at the focus shields deeper layers, further reducing the fluence available for ablation.

Although we have demonstrated the ability to create fsec LTA lesions in vitro, the number, size and location of such lesions to produce clinically significant reduction in intraocular pressure in vivo remains to be determined. Whereas Poiseuille’s law predicts that a single pore 100 μm long with a diameter of 20 μm can carry the entire aqueous outflow with a pressure decrease of 5 mmHg (Johnson and Johnson, 2001), clinical studies have suggested that the required treatment area of the TM to provide adequate trabecular outflow may be as large as 1.2 mm² (Melamed et al., 1987; Feltgen et al., 2003). The exit diameter of the lesions produced in the present study ranged from 8 to 33 μm , with corresponding Reynold’s numbers of 21–53. Although the pores were tapered, the very low Reynold’s numbers guarantee Poiseuille flow at the exit of the channels. Nevertheless, an in vivo study is clearly needed to determine whether single or multiple LTA lesions are required to obtain clinically significant intraocular pressure reduction, and in particular to determine whether the fsec LTA lesions are subject to later closure with fibrous scarring.

The optimal dimensions of a lesion depend on the region of the TM where it is created. Moreover, the variability of TM pigmentation in different patients may require different pulse energies to achieve the desired response. As noted in our study and others, the shape of the TM is triangular and thins as it approaches the cornea. The thickness of the TM ranges between 50 and 70 μm in the anterior region

and between 100 and 130 μm in the posterior portion in glaucomatous and normal eyes (Buller and Johnson, 1994; Dietlein et al., 2000; Hamard et al., 2002). Furthermore, the diameter of Schlemm’s canal is 150–300 μm (Buller and Johnson, 1994). These dimensions need to be taken into consideration when performing fsec LTA. Although we cannot predict from the present experiment the ideal laser parameters for in vivo fsec LTA, the following considerations are relevant. Ideally the laser focus should be in an area where landmarks are easily identified, where Schlemm’s canal is the widest, where the probability of collapse of Schlemm’s canal is the lowest, where there is least variability in the thickness of the meshwork, and in an area that avoids the draining aqueous channels in the outer wall of Schlemm’s canal. LTA applied to the anterior TM which is thinner would require a lower laser dosage to puncture the TM. In our experiment we achieved full thickness penetration of the TM at 0.5–2 sec at 7.2 $\mu\text{J}/\text{pulse}$ with lesions lengths varying from 50 to 87 μm . On the other hand it is possible that application of the laser in the anterior TM may cause penetration of the outer wall of Schlemm’s canal because of the narrow dimensions in this area leading to collapse and scarring of the canal.

For these reasons, the mid-meshwork (midway between the scleral spur and Schwalbe’s line) may be a reasonable location to apply fsec LTA. In this region the TM is 70–100 μm in thickness, as noted in our study and elsewhere (Dietlein et al., 2000). Moreover, Schlemm’s canal is moderately wide in this area, and the location is anterior to the aqueous drainage veins. This landmark will probably be more easily identified by using a slit-lamp-based delivery system, than by the complex viewing systems required Er:YAG and excimer LTA. We envision commercially available photonic optical fibers could deliver fsec laser energy using a slit lamp delivery system without degrading the fsec duration of the pulse in the living eye.

The optimal parameters for the present delivery system to create a lesion in this region are 0.5 sec at 14.4 $\mu\text{J}/\text{pulse}$. The mean width and depth (35 $\mu\text{m} \times 80 \mu\text{m}$) of the lesion created under these conditions appear to be sufficient to create a full thickness bypass between the anterior chamber and Schlemm’s canal. The optimal size and or number of pores created by the laser as well as the laser parameters will be determined in an in vivo experiment, where different optics will be used in the delivery system.

In this study we also demonstrated the usefulness of two-photon microscopy for quantitative measurements of thick samples of unfixed tissue. We noted that the lesion dimensions measured in the same tissue in unfixed and fixed media using two-photon microscopy differed because of shrinkage in the formaldehyde solution. This finding suggests that quantitative measurements on fixed tissue may underestimate the size of LTA lesions.

In summary, we have demonstrated the feasibility of using an 800 nm femtosecond Ti:Sapphire laser for LTA on human TM in vitro. A variety of pulse energies and exposure

times were used to create lesions in the TM with minimal collateral damage. This technique might prove to be an alternative to conventional surgery for the treatment of glaucoma following development of a slit lamp delivery system. We indicated that the optimal parameters are 14.4 $\mu\text{J}/\text{pulse}$ for 0.5 sec (at a 1 kHz repetition rate) when focused with a 0.25 NA lens onto the mid-TM.

Acknowledgements

This work was supported by the Campus Research Board of UIC, and supplemented by additional support from the Departments of Ophthalmology, Chemistry, and Bioengineering, University of Illinois at Chicago, Chicago, IL. Additionally, RJG acknowledges support from the National Science Foundation under grant numbers PHY 0200812 and CHE 0120997, and DPE acknowledges support from the NEI Core Grant EY 01792, Bethesda, MD, an unrestricted grant from Research to Prevent Blindness and William Pendill Glaucoma Research Fund.

References

- Allan, B.D., Van Saarloos, P.P., Russo, A.V., Cooper, R.L., Constable, I.J., 1993. Excimer laser sclerostomy: the in vitro development of a modified open mask delivery system. *Eye* 7, 47–52.
- Buller, C., Johnson, D., 1994. Segmental variability of the TM in normal and glaucomatous eyes. *Invest. Ophthalmol. Vis. Sci.* 35, 3841–3851.
- Campagnola, P.J., Loew, L.M., 2003. Second-harmonic imaging microscopy for visualizing biomolecular arrays in cells, tissues and organisms. *Nat. Biotechnol.* 21, 1356–1360.
- Deutsch, T.F., Geis, M.W., 1983. Self-developing UV photoresist using excimer laser exposure. *J. Appl. Phys.* 54, 7201–7204.
- Dietlein, T.S., Jacobi, P.C., Krieglstein, G.K., 1996. Erbium: YAG laser ablation on human TM by contract delivery endoprobes. *Ophthalmic Surg. Lasers* 27, 939–945.
- Dietlein, T.S., Jacobi, P.C., Schroder, R., Krieglstein, G.K., 1997. Experimental erbium: YAG laser photoablation of TM in rabbits: an in-vivo study. *Exp. Eye Res.* 64, 701–706.
- Dietlein, T.S., Philipp, C.J., Christoph, L., Günter, K.K., 2000. Morphological variability of the TM in glaucoma patients: implications for non-perforating glaucoma surgery. *Br. J. Ophthalmol.* 84, 1354–1359.
- Dietlein, T.S., Jacobi, P.C., Mietz, H., Krieglstein, G.K., 2001. Morphology of the TM three years after Erbium:YAG laser trabecular ablation. *Ophthalmic Surg. Lasers* 32, 483–485.
- Feltgen, N., Mueller, H., Ott, B., Frenz, M., Funk, J., 2003. Combined endoscopic erbium:YAG laser goniotomy and cataract surgery. *J. Cataract Refract. Surg.* 29, 2155–2162.
- Hamard, P., Valtot, F., Sourdille, P., Bourles-Dagonet, F., Baudouin, C., 2002. Confocal microscopic examination of TM removed during ab externo trabeculectomy. *Br. J. Ophthalmol.* 86, 1046–1052.
- Hill, R.A., Stern, D., Lesiecki, M.L., Hsia, J., Berns, M.W., 1993. Effects of pulse width on erbium:YAG laser photothermal trabecular ablation (LTA). *Lasers Surg. Med.* 13, 440–446.
- Huang, S., Yu, M., Feng, G., Zhang, P., Qiu, C., 2001. Histopathological study of trabeculum after excimer laser trabeculectomy ab interno. *Yan Ke Xue Bao* 17, 11–15.
- Johnson, D.H., Johnson, M., 2001. Nonpenetrating glaucoma surgery. *J. Glaucoma* 10, 55–67.
- Konig, K., 2000. Multiphoton microscopy in life sciences. *J. Microsc.* 200, 83–104.
- Lubatschowski, H., Heisterkamp, A., Will, F., Serbin, J., Bauer, T., Fallnich, C., Wellin, H., 2002. Ultrafast laser pulses for medial applications. *Proc. SPIE* 4633, 38–49.
- McHam, M.L., Eisenberg, D.L., Schuman, J.S., Wang, N., 1992. Erbium: YAG laser trabecular ablation with a sapphire optical fiber. *Exp. Eye Res.* 65, 151–155.
- Melamed, S., Pei, J., Puliafito, C.A., Epstein, D.L., 1985. Q-Switched neodymium-YAG laser trabeculopuncture in monkeys. *Arch. Ophthalmol.* 103, 129–133.
- Melamed, S., Latina, M.A., Epstein, D.L., 1987. Neodymium-YAG laser trabeculopuncture in juvenile open-angle glaucoma. *Ophthalmology* 94, 163–170.
- Mohler, W., Millard, A.C., Campagnola, P.J., 2003. Second harmonic generation imaging endogenous structural proteins. *Methods* 29, 97–109.
- Niemz, M., 2002. *Laser–Tissue Interactions*, Second Ed. Springer, Heidelberg pp. 126–149.
- Oraevsky, A.A., Da Silva, L.B., Rubenchik, A.M., Feit, M.D., Glinesky, M.E., Perry, M.D., Mammini, B.M., Small, W., Stuart, B.C., 1996. Plasma mediated ablation of biological tissues with nanosecond-to-femtosecond laser pulses: relative role of linear and nonlinear absorption. *IEEE J. Sel. Top. Quantum Electron.* 2, 801–809.
- Venkatesh, S., Lee, W.R., Guthrie, S., Cruickshank, F.R., Foulds, W.S., Quigley, R.J., Bailey, R.T., 1986. An in-vitro morphological study of Q-switched neodymium/YAG laser trabeculotomy. *Br. J. Ophthalmol.* 70, 89–96.
- Vogel, M., Lauritzen, K., 1997. Selective excimer laser ablation of the TM. Clinical results. *Ophthalmologie* 94, 665–667.
- Vogel, A., Venugopalan, V., 2003. Mechanisms of pulsed laser ablation of biological tissues. *Chem. Rev.* 103, 577–644.
- Zipfel, W.R., Williams, R.M., Christie, R., Nikitin, A.Y., Hyman, B.T., Webb, W.W., 2003. Live tissue intrinsic emission microscopy using multiphoton-excited native fluorescence and second harmonic generation. *PNAS* 100, 7075–7080.
- Zoumi, A., Yeh, A., Tromberg, B.J., 2002. Imaging cells and extracellular matrix in vivo by using second-harmonic generation and two-photon excited fluorescence. *PNAS* 99, 11014–11019.